Proceedings of the 40th IEEE
Conference on Decision and Control
Orlando, Florida USA, December 2001

On Controlling Aircraft Formations

R. Fierro[†], C. Belta[‡], J. P. Desai[*], and V. Kumar[‡]

[†]School of Electrical and Computer Engineering
Oklahoma State University, USA
rfierro@okstate.edu

[‡]GRASP Laboratory, University of Pennsylvania, USA
{calin,kumar}@grasp.cis.upenn.edu

[*]PRISM Laboratory, Drexel University, USA
desai@cbis.ece.drexel.edu

Abstract

We describe a framework for controlling a group of unmanned aerial vehicles (UAVs) flying in close formation. We first present a nonlinear dynamical model which includes the induced rolling moment by the lead aircraft on the wing of the following aircraft. Then, we outline two methods for trajectory generation of the leading aircraft, based on interpolation techniques on the Euclidean group, $SE(3)$. Two formation controllers that allow each aircraft to maintain its position and orientation with respect to neighboring UAVs are derived using input-output feedback linearization. Numerical simulations illustrate the application of these ideas and demonstrate the validity of the proposed framework.

1 Introduction

Research activity in unmanned aerial vehicles has increased substantially in the last few years. Areas of application include, space exploration [1], surveillance, target acquisition, and formation flight, see for example [2]. Researchers in *UAV* systems are facing new challenges and open issues that require deeper investigation. Single-agent techniques would require improvements and extensions to make them suitable for multiagent analysis and design. For instance, we need to address stability and robustness of multi *UAV* systems.

Flying in close formation is a hard problem which requires highly accurate sensors (*i.e.*, GPS/INS [3]), precise control systems [4], and communication/coordination protocols [5]. It is well-known that the follower aircraft can benefit from a drag reduction if it is placed on the *hot spot* of the vortex produced by its leader aircraft. However, it is also known that it is very difficult to find and maintain the airplane on such a hot spot, see for instance [6, 7].

Another important element in formation flight is trajectory generation of the lead aircraft. An attractive choice is optimal path planning on $SE(3)$ [8]. In [9], authors develop a method for generating smooth trajectories that minimize the total energy associated with the translations and rotations of the *UAV*s, while maintaining a rigid formation. If the leading aircraft is holonomic, we can generate optimal motion. For the nonholonomic case, we generate a smooth interpolant satisfying appropriate boundary conditions and nonholonomic constraints.

Two controllers have been designed based on input-output linearization. The first controller allows the following aircraft to maintain a desired position with respect to its leader. The second controller allows a third aircraft to follow two leading aircraft. Thus, a triangular formation can be maintained without collisions as the leader maneuvers along its trajectory.

The rest of the paper is organized as follows. Section 2 gives some mathematical preliminaries and formulates the formation control problem. In section 3, the nonlinear dynamical model of an aircraft is presented. The trajectory generator for the lead aircraft is outlined in section 4. Section 5 describes the basic formation controllers we use in our work. Section 6 presents some numerical simulation results and illustrates the benefits and the limitations of this methodology underlying the implementation of autonomous formation flight. Finally, some concluding remarks and future work are given in section 7.

2 Background and problem formulation

2.1 The Lie groups $SO(3)$ and $SE(3)$

Let $GL(3)$ denote the general linear group of dimension 3, which is a smooth manifold and a Lie group. The rotation group on $\mathbb{R}^3$ is a subgroup of the general linear

0-7803-7061-9/01/$10.00 © 2001 IEEE

group, defined as

$$SO(3) = \{R \,|\, R \in GL(3,\mathbb{R}),\ RR^T = I,\ \det R = 1\}$$

$GA(3) = GL(3) \times \mathbb{R}^3$ is the affine group. $SE(3) = SO(3) \times \mathbb{R}^3$ is the special Euclidean group, and is the set of all rigid displacements in $\mathbb{R}^3$. Special consideration will be given to $SO(3)$ and $SE(3)$. The Lie algebras of $SO(3)$ and $SE(3)$, denoted by $so(3)$ and $se(3)$ respectively, are given by:

$$so(3) = \left\{\hat{\omega} \in \mathbb{R}^{3\times 3},\ \hat{\omega}^T = -\hat{\omega}\right\},$$

$$se(3) = \left\{ \begin{bmatrix} \hat{\omega} & v \\ 0 & 0 \end{bmatrix} \,|\, \hat{\omega} \in so(3), v \in \mathbb{R}^3 \right\}$$

where $\hat{\omega}$ is the skew-symmetric matrix form of the vector $\omega \in \mathbb{R}^3$. Given a curve

$$A(t) : [-a, a] \to SE(3),\ A(t) = \begin{bmatrix} R(t) & d(t) \\ 0 & 1 \end{bmatrix} \quad (1)$$

an element $\zeta(t)$ of the Lie algebra $se(3)$ can be associated to the tangent vector $\dot{A}(t)$ at an arbitrary point t by:

$$\zeta(t) = A^{-1}(t)\dot{A}(t) = \begin{bmatrix} \hat{\omega}(t) & R^T\dot{d} \\ 0 & 0 \end{bmatrix} \quad (2)$$

where $\hat{\omega}(t) = R^T\dot{R}$ is the corresponding element from $so(3)$. Consider a rigid body moving in free space. Assume any inertial reference frame $\{E\}$ fixed in space and a frame $\{B\}$ fixed to the body at point O as shown in Figure 1. A curve on $SE(3)$ physically represents a motion of the rigid body. If $\{\omega(t), v(t)\}$ is the vector pair corresponding to $\zeta(t)$, then ω corresponds to the angular velocity of the rigid body while v is the linear velocity of O, both expressed in the frame $\{B\}$. In kinematics, elements of this form are called twists and $se(3)$ thus corresponds to the space of twists. The twist $\zeta(t)$ computed from Equation (2) does not depend on the choice of the inertial frame.

In this paper, we use Euler angles body fixed ZYX as parameterization of $SO(3)$. Explicitly, the rotation $R(\phi, \theta, \psi)$ is composed of a rotation of ψ about the z-axis, followed by a rotation of θ about the y-axis, and a rotation of ϕ about the x-axis.

2.2 Problem formulation

We formulate the autonomous formation flight problem as a three-level hierarchy. The trajectory generator produces a trajectory $A(t) \in SE(3)$ for the lead aircraft to follow. Then, the coordination protocol provides the desired set-point values to the control level. Finally, controllers based on input-output feedback linearization allow the aircraft $\mathcal{A}_j$ to follow its designated leader $\mathcal{A}_i$.

In general, we would like to place each follower on the *hot spot* of the vortex produced by its leader, thus a maximum drag reduction for the group is achieved. If in addition we generate a smooth leading trajectory, then the whole formation will *flow* describing a well-behaved motion in terms of fuel consumption.

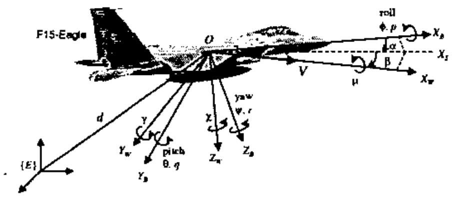

Figure 1: Body reference frames on an aircraft.

3 Aircraft Nonlinear Model

In this section, we describe the dynamical model of an aircraft. As it is shown in Figure 1, the angles $(\mu,\ \gamma,\ \chi)$ describe the attitude with respect to the ***wind axes***, $(p,\ q,\ r)$ are the components of the angular velocity ω_b with respect to the body frame (these components are usually referred as ***roll rate***, ***pitch rate***, and ***yaw rate***). V is the aircraft velocity, and α, β are the angles of attack and sideslip, respectively. The notation commonly used in flight dynamics [10] is summarized in Table 1. The range of values of the Euler angles is

Table 1: ZYX Euler Angles

Axes	roll θ_x	pitch θ_y	yaw θ_z
Wind	μ	γ	χ
Body	ϕ	θ	ψ
Stability	0	α	$-\beta$

$$-\pi \le \theta_x < \pi, \qquad -\frac{\pi}{2} \le \theta_y \le \frac{\pi}{2}, \qquad 0 \le \theta_z < 2\pi.$$

The equations of motion of an aircraft are given by

$$\dot{V} = -\frac{D}{m} - g\sin\gamma \quad (3)$$

$$\dot{\alpha} = q - q_w \sec\beta - (p\cos\alpha + r\sin\alpha)\tan\beta \quad (4)$$

$$\dot{\beta} = r_w + p\sin\alpha - r\cos\alpha \quad (5)$$

where m is the mass of the aircraft and g is the gravity constant. The components of the angular velocity in ***wind*** frame become

$$p_w = (p\cos\alpha + r\sin\alpha)\cos\beta + (q - \dot{\alpha})\sin\beta$$

$$q_w = \frac{1}{mV}(L - mg\cos\mu\cos\gamma)$$

$$r_w = \frac{1}{mV}(-C + mg\sin\mu\cos\gamma)$$

The input vector is $u = [\delta_p \quad \delta_a \quad \delta_e \quad \delta_r]^T$ where δ_p denotes the setting of the ***throttle***, and $(\delta_a,\ \delta_e,\ \delta_r)$ denote the deflections of the ***aileron***, ***elevator***, and ***rudder***, respectively.

The roll, pitch and yaw rates in wind axes become

$$\dot{\mu} = p_w + (q_w \sin\mu + r_w \cos\mu)\tan\gamma \quad (6)$$
$$\dot{\gamma} = q_w \cos\mu - r_w \sin\mu \quad (7)$$
$$\dot{\chi} = (q_w \sin\mu + r_w \cos\mu)\sec\gamma \quad (8)$$

If the angular velocity with respect to the body frame is $\omega_b = [p \quad q \quad r]^T$, then

$$\dot{\omega}_b = \begin{pmatrix} \dot{p} \\ \dot{q} \\ \dot{r} \end{pmatrix} = J_b^{-1}\hat{\omega}_b J_b \omega_b + J_b^{-1}\tau + \mathcal{L} \quad (9)$$

where J_b is the inertia matrix, $\hat{\omega}_b$ is the skew-symmetric operator, τ is the external moment vector, and $\mathcal{L} = [L_p \quad 0 \quad 0]^T$ is the rolling moment induced by the wake of the *lead* aircraft [11, 12]. The vortex produces an *up-wash* on the wing of the following aircraft. As a result, the angle of attack and the lift increase. Since the vortex-induced velocity decreases with distance, L_p is generated. It is assumed here that L_p can be estimated using an appropriate filter [6]. For a detailed introduction on formation flight aerodynamics, the reader is referred to [4].

The aerodynamic forces $F_w = [-D \; -C \; -L]^T$ are the *drag*, *side*, and *lift*, respectively, and the external moments acting on the aircraft are $\tau = [L_\phi \quad M_\theta \quad N_\psi]^T$. Forces and moments are nonlinear vector functions of the aerodynamic parameters, the *maximal thrust* $\mathcal{P}$, the input vector, and the state of the aircraft. It is assumed that the thrust has no effect on τ, and the deflections (δ_a, δ_e, δ_r) have no effect on F_w.

By using the flat non-rotating Earth assumption, the *wind-axis navigation* equations expressed on Earth reference frame $\{E\}$ become

$${}^E\dot{x} = V\cos\gamma\cos\chi \quad (10)$$
$${}^E\dot{y} = V\cos\gamma\sin\chi \quad (11)$$
$${}^E\dot{z} = -V\sin\gamma \quad (12)$$

Equations (3)–(12) describe an aircraft whose state $\boldsymbol{X} \equiv [X_{\text{long}}^T \quad X_{\text{lat}}^T]^T$ is defined in an open neighborhood $\boldsymbol{X} \subset \mathbb{R}^{12}$, where

$$X_{\text{long}} = [V \quad \alpha \quad q \quad \gamma \quad {}^E x \quad {}^E z]^T \quad (13)$$
$$X_{\text{lat}} = [\beta \quad p \quad r \quad \mu \quad \chi \quad {}^E y]^T \quad (14)$$
$$u = [\delta_p \quad \delta_a \quad \delta_e \quad \delta_r]^T \quad (15)$$

are the longitudinal and lateral state vectors, and the input vector, respectively.

In the next section we describe the trajectory generator for the lead aircraft.

4 Trajectory Generation on $SE(3)$

4.1 Optimal trajectory generation for a holonomic aircraft

If J_b is the inertia matrix of the airplane about frame $\{B\}$ placed at the centroid and m is its mass, then the total kinetic energy of the moving airplane induces a left invariant metric on $SE(3)$. If A is an arbitrary point on $SE(3)$ and $X, Y \in T_A SE(3)$, then

$$< X, Y >_{SE} = \left[\begin{array}{cc} \omega_x^T & v_x^T \end{array} \right] \tilde{G} \left[\begin{array}{c} \omega_y \\ v_y \end{array} \right], \quad (16)$$
$$\tilde{G} = \left[\begin{array}{cc} J_b/2 & 0 \\ 0 & m/2I_3 \end{array} \right]$$

where $\{\omega_x, v_x\}$ is the vector representation of the twist corresponding to X. Metric (16) can be shown to be inherited from the ambient space $GA(3)$, where the metric has the following form:

$$< X, Y >_{GA} = Tr(X^T Y \tilde{W}) \quad (17)$$

with

$$\tilde{W} = \left[\begin{array}{cc} W & 0 \\ 0 & 1/2m \end{array} \right], \; W = \frac{1}{4}Tr(J_b)I_3 - \frac{1}{2}J_b; \quad (18)$$

We can use the norm induced by metric (17) to define the distance between elements in $GA(3)$. Using this distance, for a given $B \in GA(3)$, we define *the projection* of B on $SE(3)$ as being the closest $A \in SE(3)$ with respect to metric (17). The following result is stated and proved in [13]:

Proposition 4.1 *Let $B \in GA(3)$ with the following block partition*

$$B = \left[\begin{array}{cc} B_1 & B_2 \\ 0 & 1 \end{array} \right], \; B_1 \in GL(3), \; B_2 \in \mathbb{R}^3$$

and U, Σ, V the singular value decomposition of $B_1 W$:

$$B_1 W = U \Sigma V^T \quad (19)$$

Then the projection of B on $SE(3)$ is given by

$$A = \left[\begin{array}{cc} UV^T & B_2 \\ 0 & 1 \end{array} \right] \in SE(3) \quad (20)$$

Based on Proposition 4.1, a procedure for generating near optimal curves on $SE(3)$ follows: generate the curves in $GA(3)$ and project them on $SE(3)$. In [13], we prove that the overall procedure is left invariant (*i.e.*, the generated trajectories are independent of the choice of the inertial frame $\{E\}$). The projection method can be used to generate near optimal interpolating motion between end poses (geodesics) or poses and velocities (minimum acceleration curves). In what follows, the given boundary conditions will be denoted by $R^0, d^0, \dot{R}^0, \dot{d}^0$ at $t = 0$ and $R^1, d^1, \dot{R}^1, \dot{d}^1$ at $t = 1$.

The differential equations to be satisfied by geodesics on $SE(3)$ equipped with metric (16) are derived in [14]. The translational part is easily integrable: $d(t) = d^0 + (d^1 - d^0)t,\ t \in [0,\ 1]$ If the projection method is used, the rotation is given by $R(t) = U(t)V^T(t)$, where $M(t)W = U\Sigma V^T$ with $M(t) = [R^0 + (R^1 - R^0)t]W$.

4.2 Trajectory generation for a nonholonomic leader

In this section we assume that the leader is a nonholonomic (airplane like) aircraft, whose velocity is always along the x-axis of its body frame $\{B\}$. Given the motion of its centroid $d(t)$ in the earth frame $\{E\}$, we generate the airplane's rotation so that the nonholonomic constraint is satisfied at all times.

A nice solution to this problem can be found using controls as in [15]. Alternatively, let $d(t) \in \mathbb{R}^3$ be a smooth curve describing the translational part of $A(t) \in SE(3)$ as in (1). We need to generate the rotational part $R(t) \in SO(3)$ so that the velocity $\dot{d}(t)$ is along the x-axis of the moving frame $\{B\}$. For motion planning, we assume that the body frame $\{B\}$ is coincident with the wind frame $\{W\}$. Let $n(t) = [n_x\ n_y\ n_z]^T$ be the unit vector along the velocity $\dot{d}(t)$, *i.e.*, $n(t) = d(t)/\|\dot{d}(t)\|$. Then, by definition of a rotation matrix, $n(t)$ should be the first column of $R(t)$. Using $R(\phi, \theta, \psi)$ and following the notation in Table 1, $\chi(t)$ and $\gamma(t)$ are easily determined. The third angle $\mu(t)$ can be arbitrarily chosen, for example, as a linear function of time to interpolate between given end poses.

5 *UAV* Formation Control

By following the lines of [16], we would like to use dynamic feedback and coordinate transformation to convert the nonlinear system (3)–(12) into a fully linear system. The state vector $\boldsymbol{X}$ is rearranged into the following four subsets

$$x_1 = (V,\ \gamma,\ \chi) \quad (21)$$
$$x_2 = (\mu,\ \alpha,\ \beta) \quad (22)$$
$$x_3 = (p,\ q,\ r) \quad (23)$$
$$x_4 = ({}^E x,\ {}^E y,\ {}^E z) \quad (24)$$

Similarly for the input commands, we have

$$u_1 = \delta_p \quad (25)$$
$$u_2 = (\delta_a,\ \delta_e,\ \delta_r) \quad (26)$$

Now we derive a controller for the follower aircraft $\mathcal{A}_j$ assuming the lead aircraft $\mathcal{A}_i$ is tracking $A(t) \in SE(3)$. Thus, $\mathcal{A}_j$ should maintain a prescribed *relative* position and orientation with respect to its leader $\mathcal{A}_i$. As usual, the control objective is to drive the output vector $\|z^d - z\| \to 0$ as $t \to \infty$. The desired output z^d will depend on the desired formation shape.

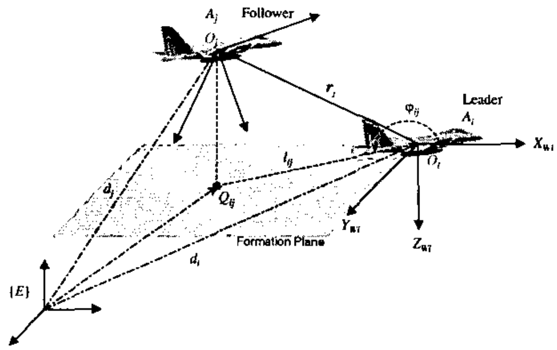

Figure 2: Flight formation geometry.

The geometry of two *UAV*s flying in formation is depicted in Figure 2. The plane formed by the X_{W_i} and Y_{W_i} wind axes of the lead aircraft is called *formation plane*. Let Q_{ij} denote the projection of the center of mass of $\mathcal{A}_j$ on the formation plane of $\mathcal{A}_i$. If we can control the relative altitude ${}^i z_j$, then the control problem reduces to control the position of Q_{ij}. The relative position of Q_{ij} is specified by the separation l_{ij} and bearing φ_{ij}. Similarly, Q_{ij} can be defined by the relative positions ${}^i x_j$, ${}^i y_j$ in the leader's frame $\{i\}$. The fourth selected output variable is the relative roll angle μ_{ij}, since the main effect of the flying in close formation is the induced rolling moment on the wingman. Thus, the output vector becomes

$$z_{ij} = \begin{bmatrix} {}^i x_j & {}^i y_j & {}^i z_j & \mu_{ij} \end{bmatrix}^T \quad (27)$$

where

$$\begin{pmatrix} {}^i x_j \\ {}^i y_j \\ {}^i z_j \\ 1 \end{pmatrix} = {}^i A_E \begin{pmatrix} {}^E x_j \\ {}^E y_j \\ {}^E z_j \\ 1 \end{pmatrix}$$
$$\mu_{ij} = \mu_i - \mu_j$$

where ${}^i A_E$ denotes the transformation matrix from $\{E\}$ to $\{i\}$. The output vector can be rewritten as $z_{ij} = \begin{bmatrix} \bar{x}_{4_{ij}} & \mu_{ij} \end{bmatrix}^T$. Moreover, we have

$$\dot{\bar{x}}_{4_{i,j}} = F_4(x_{1_j}, \boldsymbol{X}_i) \quad (28)$$

F_4 is a nonlinear vector function, x_{1_j} is given in (21), and $\boldsymbol{X}_i$ is the state vector of the leader treated as an exogenous input. Applying input-output feedback linearization via dynamic extension, it can be shown that system (21)–(23) with input (25)–(26), and output (27) is transformed into a linear and controllable system given by

$${}^i x_j^{(4)} \equiv z_{1_{ij}}^{(4)} = \bar{w}_1 \quad (29)$$
$${}^i y_j^{(4)} \equiv z_{2_{ij}}^{(4)} = \bar{w}_2 \quad (30)$$
$${}^i z_j^{(4)} \equiv z_{3_{ij}}^{(4)} = \bar{w}_3 \quad (31)$$
$$\ddot{\mu}_{ij} \equiv \ddot{z}_{4_{ij}} = \bar{w}_4 \quad (32)$$

The extended system (29)–(32) is $14th$ dimensional. The auxiliary input vector $\bar{w}$ is designed by well-known linear control design methods. For a relative separation distance (*e.g.*, ${}^ix_j$) and relative roll angle, we have

$$\begin{aligned}\bar{w}_1 &= {}^ix_j^{(4)d} + k_{11}({}^ix_j^{(3)d} - {}^ix_j^{(3)}) + k_{12}({}^i\ddot{x}_j^d - {}^i\ddot{x}_j) \\ &\quad + k_{13}({}^i\dot{x}_j^d - {}^i\dot{x}_j) + k_{14}({}^ix_j^d - {}^ix_j) \\ \bar{w}_4 &= \ddot{\mu}_{ij}^d + k_{41}(\dot{\mu}_{ij}^d - \dot{\mu}_{ij}) + k_{42}(\mu_{ij}^d - \mu_{ij})\end{aligned}$$

where k_{ab}'s are design parameters.

In order to achieve the maximum drag reduction on $\mathcal{A}_j$, a precise close formation control is required [17, 12]. In [11], authors showed that an optimal geometry can be obtained if $\mathcal{A}_j$ is placed on the formation plane of $\mathcal{A}_i$ (*i.e.*, ${}^iz_j = 0$), and ${}^ix_j \approx 3b$, ${}^iy_j \approx \frac{\pi}{4}b$. $b = 10$ m. is the leader's wingspan used in our simulation experiments.

We will use these specifications to design two basic formation controllers that allow three aircraft $\mathcal{A}_{i,j,k}$ to maintain a triangle formation as the leader $\mathcal{A}_i$ maneuvers along $A(t) \in SE(3)$, see Figure 3. Assuming we can regulate the relative altitudes about $z^d_{3_{ij}} = 0$ and $z^d_{3_{ik}} = 0$, then we need to control the relative separations l_{ij}, l_{ik}, and bearings φ_{ij}, φ_{ik} to keep the desired formation shape. Similar controllers have been derived in our previous work for the case of on ground autonomous vehicles [18, 19].

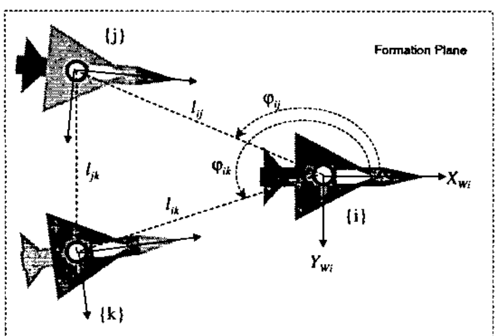

Figure 3: Three aircraft in a triangle formation.

5.1 Controller I

By using this controller, aircraft $\mathcal{A}_j$ follows $\mathcal{A}_i$ with desired separation $z^d_{1_{ij}}$ and $z^d_{2_{ij}}$. Similarly, $\mathcal{A}_k$ follows $\mathcal{A}_i$ with desired separation $z^d_{1_{ik}}$ and $z^d_{2_{ik}}$.

The linearized closed–loop dynamics are given by

$$\begin{aligned} z^{(4)}_{1_{ij}} &= \bar{w}_{1j}, \qquad z^{(4)}_{2_{ij}} = \bar{w}_{2j}, && (33)\\ z^{(4)}_{3_{ij}} &= \bar{w}_{3j}, \qquad \ddot{z}_{4_{ij}} = \bar{w}_{4j} \\ z^{(4)}_{1_{ik}} &= \bar{w}_{1k}, \qquad z^{(4)}_{2_{ik}} = \bar{w}_{2k}, && (34)\\ z^{(4)}_{3_{ik}} &= \bar{w}_{3k}, \qquad \ddot{z}_{4_{ik}} = \bar{w}_{4k}\end{aligned}$$

Since there is no interaction/communication between the followers $\mathcal{A}_j$ and $\mathcal{A}_k$, collisions (*i.e.*, $l_{jk} < \delta_{\text{safe}}$ in Figure 3) may occur for some initial conditions or leader's trajectories. It is important to realize that stability of each agent in formation is a necessary but not a sufficient condition for successfully accomplishing a formation task. However, this limitation can be overcome by directly controlling the separation between $\mathcal{A}_j$ and $\mathcal{A}_k$ as it is shown next.

5.2 Controller II

In this case, aircraft $\mathcal{A}_j$ follows $\mathcal{A}_i$ with desired separation $z^d_{1_{ij}}$ and $z^d_{2_{ij}}$. However, $\mathcal{A}_k$ follows both $\mathcal{A}_i$ and $\mathcal{A}_j$ with desired separation l^d_{ik} and l^d_{jk}. Thus the relative desired position of the third aircraft will depend on the state of both $\mathcal{A}_i$ and $\mathcal{A}_j$. Suppose the follower $\mathcal{A}_j$ is commanded to change its position with respect to the lead *UAV*, then $\mathcal{A}_k$ will also update its position accordingly.

As before, the linearized closed–loop dynamics can be expressed as

$$\begin{aligned} z^{(4)}_{1_{ij}} &= \bar{w}_{1j}, \qquad z^{(4)}_{2_{ij}} = \bar{w}_{2j}, && (35)\\ z^{(4)}_{3_{ij}} &= \bar{w}_{3j}, \qquad \ddot{z}_{4_{ij}} = \bar{w}_{4j} \\ z^{(4)}_{1_{(i,j)k}} &= \bar{w}_{1k}, \qquad z^{(4)}_{2_{(i,j)k}} = \bar{w}_{2k}, && (36)\\ z^{(4)}_{3_{ik}} &= \bar{w}_{3k}, \qquad \ddot{z}_{4_{ik}} = \bar{w}_{4k}\end{aligned}$$

If the leader's trajectory is well-behaved, then the three–aircraft system maintains formation and no collisions will occur.

6 Simulation Results

We illustrate our approach using three F-16 like aircraft $\mathcal{A}_i$, $\mathcal{A}_j$ and $\mathcal{A}_k$ flying in close formation. Initially, the lead *UAV* is flying at an altitude of ${}^Ez_{i0} = 12000$ m, $V_{i0} = 250$ m/s and roll $\mu_{i0} = 15°$. It is commanded to reach an altitude of ${}^Ez_{if} = 15000$ m, $V_{if} = 250$ m/s and roll $\mu_{if} = 30°$. Then, the lead trajectory $A(t) \in SE(3)$ is generated by the method outlined in section 4. The desired separation distances and relative roll angles for the followers are (${}^ix^d_j = -30$ m, ${}^iy^d_j = -12$ m, ${}^iz^d_j = 0$ m, $\mu^d_{ij} = 0°$) and (${}^ix^d_k = -30$ m, ${}^iy^d_k = 12$ m, ${}^iz^d_j = 0$ m, $\mu^d_{ij} = 0°$), respectively. As it can be seen in Figure 4 the relative position variables converge asymptotically to the desired values. Figure 5 depicts the $3D$ trajectories described by the group of *UAV*s flying in close formation. The plot has been properly re-scaled for visualization purposes. *Controller I* drives each follower to the leader's formation plane. *Controller II* has similar performance; therefore, simulation results are omitted here.

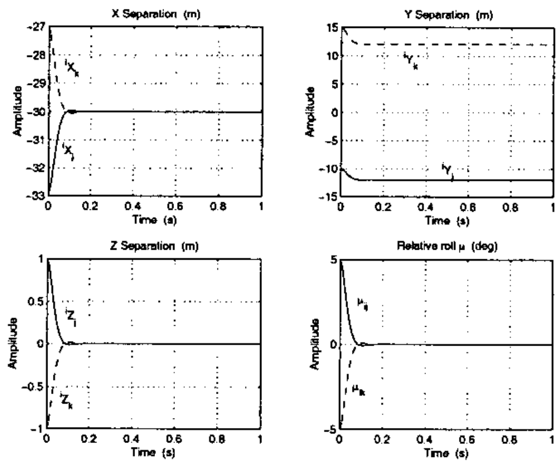

Figure 4: Controlled output variables of follower *UAVs*.

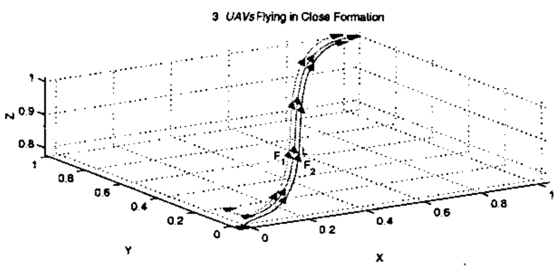

Figure 5: Three aircraft in formation.

7 Conclusions

In this paper, we have introduced a framework for autonomous formation flight. We have integrated two fundamental components in formation control of *UAVs*: trajectory generation for the lead aircraft, and a set of controllers based on input-output feedback linearization for the following *UAVs*. The framework described here can also be applied to other types of unmanned vehicles (*e.g.*, helicopters, spacecraft, and underwater vehicles). Currently, we are deriving a suite of stable control laws that provides more flexibility and safety in formation flight missions. In addition, we are developing a coordination/communication protocol that allows the aircraft change formations by switching control laws in a stable fashion.

References

[1] A. Roberson, G. Inalhan, and J. How, "Formation control strategies for a separated spacecraft interferometer," in *Proc. American Control Conference*, San Diego, CA, June 1999, pp. 4142–4147.

[2] D. Schoenwald, "Autonomous unmanned vehicles: In space, air, water, and on the ground," *IEEE Control Systems*, vol. 20, no. 6, pp. 15–18, 2000.

[3] W. Williamson, J. Min, J. Speyer, and J. Farrel, "A comparison of state space, range space, and carrier phase differential gps/ins relative navigation," in *Proc. American Control Conf.*, Chicago, IL, June 2000, pp. 2932–2938.

[4] J. D. Wolfe, D. F. Chichka, and J. L. Speyer, "Decentralized controllers for unmanned aerial vehicle formation flight," in *Proc. AIAA Guidance, Navigation, and Control Conf.*, San Diego, CA, August 1996.

[5] F. Giulietti, L. Pollini, and M. Innocenti, "Autonomous formation flight," *IEEE Control Systems*, vol. 20, no. 6, pp. 34–44, 2000.

[6] D. F. Chichka, J. L. Speyer, and C. G. Park, "Peak-seeking control with application to formation flight," in *Proc. IEEE Conf. Decision and Control*, Phoenix, AZ, December 1999, pp. 2463–2470.

[7] S. Singh, P. Chandler, C. Schumacher, S. Banda, and M. Pachter, "Adaptive feedback linearizing nonlinear close formation control of uavs," in *Proc. American Control Conf.*, Chicago, IL, June 2000, pp. 854–858.

[8] G. Walsh, R. Montgomery, and S. Sastry, "Optimal path planning on matrix lie groups," in *Proc. IEEE Conf. Decision Contr.*, Lake Buena Vista, FL, Dec. 1994, pp. 1258–1263.

[9] C. Belta and V. Kumar, "Motion generation for formations of robots: a geometric approach," in *Proc. IEEE Int. Conf. Robot. Automat.*, Seoul, Korea, May 2001, pp. 1245–1250.

[10] W. C. Durham, "Aircraft dynamics & control," Virginia Polytechnic Institute, 1997.

[11] W. Blake and D. Multhopp, "Design, performance and modeling considerations for close formation flight," in *Proc. AIAA Guidance, Navigation and Control Conf.*, Boston, MA, July 1998, Paper No. 98-4343.

[12] A. Proud, M. Pachter, and J. D'Azzo, "Close formation flight control," in *Proc. AIAA Guidance, Navigation and Control Conf.*, Portland, OR, August 1999, vol. 2, pp. 1231–1246, Paper No. 99-4207.

[13] C. Belta and V. Kumar, "New metrics for rigid body motion interpolation," in *Ball 2000 Symposium Commemorating the Legacy, Works, and Life of Sir Robert Stawell Ball*, University of Cambridge, UK, 2000.

[14] M. Žefran, V. Kumar, and C. Croke, "On the generation of smooth three-dimensional rigid body motions," *IEEE Transactions on Robotics and Automation*, vol. 14, no. 4, pp. 576–589, 1998.

[15] P. Tabuada and P. Lima, "Position tracking for underactuated rigid bodies on $se(3)$," in *Proc. 5th IFAC Symposium on Nonlinear Control Systems, NOLCOS'2001*, Saint Petersburg, July 2001.

[16] A. Isidori, *Nonlinear Control Systems*, Springer-Verlag, London, 3rd edition, 1995.

[17] J. Hall and M. Pachter, "Formation maneuvers in three dimensions," in *Proc. IEEE Conference on Decision and Control*, Sydney, December 2000, pp. 364-369.

[18] J. Desai, J. P. Ostrowski, and V. Kumar, "Controlling formations of multiple mobile robots," in *Proc. IEEE Int. Conf. Robot. Automat.*, Leuven, Belgium, May 1998, pp. 2864–2869.

[19] R. Fierro, A. Das, V. Kumar, and J. P. Ostrowski, "Hybrid control of formations of robots," *Proc. IEEE Int. Conf. Robot. Automat., ICRA01*, pp. 157–162, May 2001.